INVESTIGATION OF FACTORS THAT INFLUENCE CREEP CORROSION ON PRINTED CIRCUIT BOARDS

Haley Fu
iNEMI, Shanghai, China
haley.fu@inemi.org

Cherie Chen
IST-Integrated Service Technology, Inc., Hsinchu, Taiwan
Cherie_chen@istgroup.com

Prabjit Singh and Jing Zhang
IBM Corporation, Poughkeepsie, NY, USA
pjsingh@us.ibm.com and jingzhan@us.ibm.com

Anil Kurella
Intel Corporation, Hillsboro, OR, USA
anil.k.kurella@intel.com

Xu Chen
Alcatel-Lucent, Murray Hill, NJ, USA
chenxu@alcatel-lucent.com

Xiaodong Jiang
Alcatel Shanghai Bell, Shanghai, PR China
xiaodong.jiang@alcatel-sbell.com.cn

Jennifer Burlingame
Cisco Corporation, San Jose, CA, USA
jburling@cisco.com

Simon Lee
The Dow Chemical Company, Tao Yuan Hsien, Taiwan
simonlee@dow.com

ABSTRACT

Test printed circuit test boards (PCBs) with various surface finishes were subjected to a mixed flowing gas environment with gaseous composition adjusted to achieve a targeted 500-600 nm/day copper corrosion rate. Board surface finishes included immersion silver (ImAg), organic solderability preservative (OSP) and lead-free hot-air-solder leveling (Pb-free HASL). The PCB test specimens were prepared by reflowing lead-free solder paste on the top side and wave soldering the bottom side with lead-free solder using no-clean organic acid flux on some specimens and no-clean rosin flux on others. The solder paste contained rosin flux with low activity and zero halides. Copper creep corrosion was observed mainly on the ImAg finished boards that were wave soldered with no-clean organic acid flux. Pb-free HASL finished boards that were wave soldered with no-clean organic acid flux experienced some severe but localized creep corrosion due to exposed copper metallization and possibly flux residues from the Pb-free HASL or assembly operations. Creep corrosion was most severe in the wave soldered boundary areas where flux residue was present. Circuit boards wave soldered with no-clean rosin flux had insignificant creep corrosion.
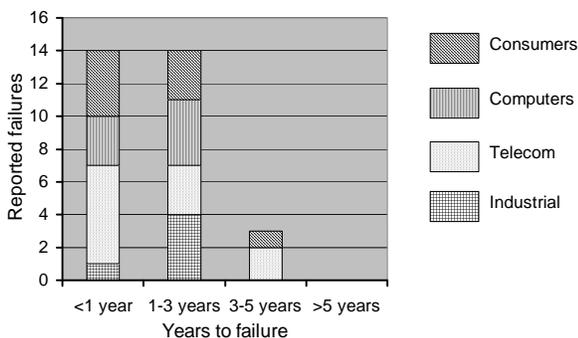
INTRODUCTION

Ever since the dawn of the electronics age, lead-tin solder has been successfully used for printed circuit board (PCB) assemblies. Lead-tin solder wets copper metallization on PCBs well and is resistant to corrosion even in very harsh environments. The adoption of the European Union Restriction of Hazardous Substance (RoHS) directive in February 2003 and its taking effect on 1 July 2006 [1]
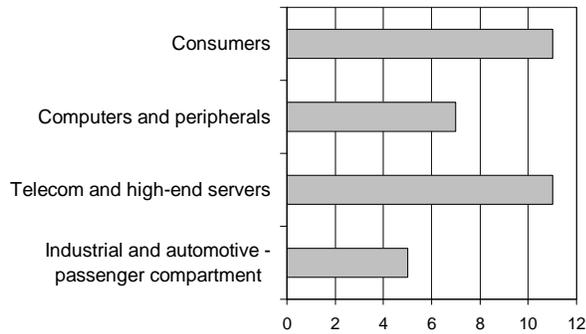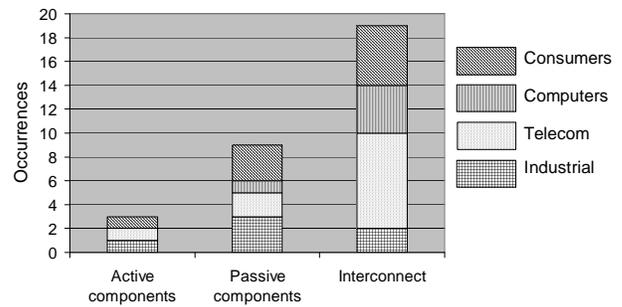
Figure 1: Creep corrosion survey completed in December 2009 showing number of respondents with creep corrosion in each product type.

Figure 3: Location of creep corrosion failures.

changed the dominance of Pb-Sn solder in the electronics industry. The Pb-free solders that replaced Pb-Sn typically contain tin (Sn), silver (Ag) and copper Cu) and are known for short as SAC solders. Unlike Pb-Sn solder, SAC solder wets copper poorly and the wettability suffers dramatically with storage time. Even before the change to Pb-free solder was contemplated, industry was busy improving PCB coplanarity necessitated by hardware miniaturization trends. Many different surface treatments were considered including immersion silver (ImAg), organic solderability preservative (OSP), electroless nickel immersion gold (ENIG), immersion tin (ImSn) and Pb-free hot air solder leveling (Pb-free HASL). In early 2000's, ImAg came into vogue, but today, ENIG, OSP and HASL dominate the market followed by ImAg and ImSn. Relative to Pb-free technology, Pb-Sn solder technology has suffered less from creep corrosion. The move to SAC soldered PCBs was not considered different enough to warrant a thorough industry-wide study. A taskforce, that later became the IPC 3-11g Metal Finishes Data Acquisition Group, worked with Underwriters Laboratories (UL) and proposed an exemption to the UL-796 test for electrochemical migration. Extensive testing had demonstrated that electrochemical migration was not an issue with ImAg. Unfortunately, no one had raised the concern that creep corrosion may occur on the new board finishes coming online, even though creep corrosion failure mode was known to occur on integrated-circuit plastic packages and on gold- and palladium-plated electrical contacts [3]. Creep corrosion is the corrosion of copper/silver metallization and

the spread of the sulfide corrosion product across the surface of the PCB. Failure may occur if the sulfide corrosion product bridges and thus electrically shorts the neighboring features on a PCB. The first reported evidence of creep corrosion on PCBs was probably by Veale in 2005 [4]. Creep corrosion failure of Pb-free ImAg boards was reported in industrial environments high in sulfur-bearing gaseous pollution. Following the creep corrosion experience in the field, Veale subjected test boards with various finishes to mixed-flowing gas (MFG) environment [5] and reported that no Pb-free board would survive Instrument Society of Automation (ISA) 71.04-1985 severity level G3 [6] and that ENIG and ImAg boards will not even survive ISA severity level G2. In 2005, Cullen [7] reported that typical MFG environment testing did not produce creep corrosion on Pb-free PCBs. The first reported creep corrosion on PCBs in computer hardware was probably by Mazurkiewicz [8] who in 2006 reported that the move to ImAg and OSP board finishes, motivated by compliance to RoHS, dramatically increased the computer early life failures due to copper creep corrosion emanating from exposed copper on PCBs, especially inside the plated-through barrels. The lack of awareness of creep corrosion was highlighted in a 2007 paper by Schueller [9] that Pb-free desktops that had been thoroughly qualified with a regimen of tests started failing in the field within 2-4 months of being put in service.

The awareness that creep corrosion on Pb-free PCBs is
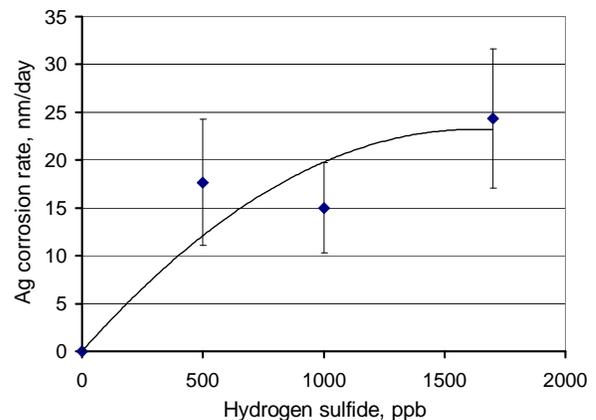

Figure 2: Time to creep corrosion failure.
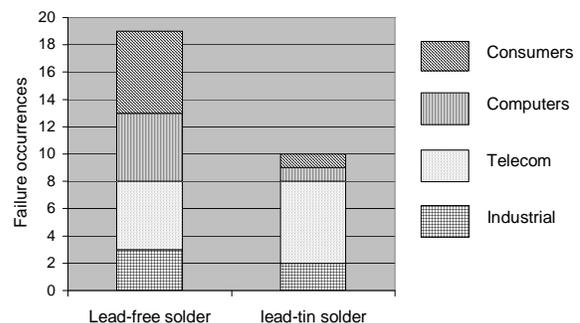
Figure 4: Distribution of creep corrosion failures.
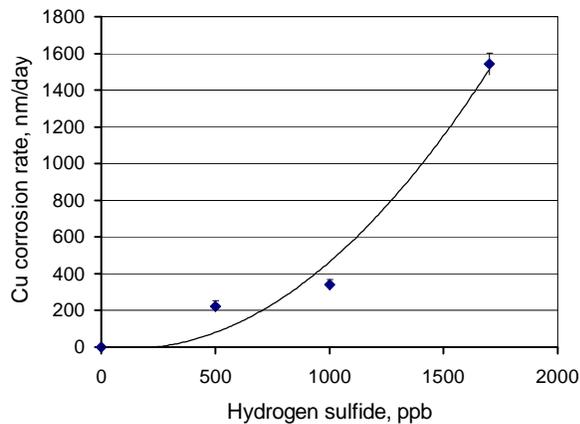
Figure 5: Copper corrosion rate in MFG chamber. The error bars representing one standard deviation bars are barely visible.

Figure 6: Silver corrosion rate in MFG chamber. The error bars shown are for one standard deviation.

highly surface sensitive was reported by Xu et. al. in 2007 and 2009 **[10, 11]**. The work reported the following general observations: PCBs with clean FR4 and clean solder mask surfaces were found not to support creep corrosion; Organic acid wave soldering flux residues supported creep corrosion; Rosin-based wave soldering fluxes and rosin-based solder paste are resistant to creep corrosion; MFG testing provides a realistic accelerated test for creep corrosion.

The restriction on the use of lead in solders in electronics occurred as the electronic market in the Far East was expanding at a rapid rate. The combination of the poor corrosion resistance of the Pb-free PCB assemblies and the greater proliferation of electronics in the Far Eastern geographies, high in sulfur-bearing gaseous pollution, led to a dramatic rise in the PCB failure rates due to creep corrosion. Suddenly, there arose a need for a corrosion test to qualify products that could survive the harsh sulfur-bearing environments and there arose a need to define a reasonable level of gaseous contamination in which electronics should be able to operate reliably. Various technical committees, including those of ASHRAE, IPC, ISA and iNEMI became active in this arena.

ASHRAE conducted a worldwide survey of the corrosion rates of copper and silver in data centers with and without creep corrosion failures and concluded that for the environment to be acceptable for modern electronics, the rate of silver corrosion should be less than 200 angstroms/month and that of copper should be less than 300 angstroms/month. ASHRAE published a white paper on the subject in 2009 and revised it in 2011 **[12]**.

The challenge remains to develop a test that suppliers of Pb-free PCB assemblies can use to satisfy their customers that their products will survive reasonably clean environments defined in the 2011 ASHRAE white paper as having silver and copper corrosion rates less than 200 and 300 angstroms/month, respectively. To this end, a three-phase iNEMI taskforce was established in 2009 to study creep corrosion on PCBs. Phase 1, completed in 2009, consisted of surveying the creep corrosion field failures. Phase 2 used the output of phase 1 to analyze and understand the root cause of creep corrosion. The taskforce is presently working on phase 3 investigating the factors influencing creep corrosion by subjecting test PCBs to MFG environments. This paper describes the results of phase 1 and 2 and the results of the partially completed phase 3.

iNEMI PROJECT DESCRIPTION
In phase 1, iNEMI conducted a world-wide creep corrosion survey to collect data on the affected products and components, the time to failure and the solder metallurgies influencing the corrosion. The four different product types surveyed were industrial and automotive, telecom and high-end servers, computers and peripherals and consumer products. Of the 45 respondents, 67% reported creep corrosion failures. The failure distribution amongst the four product groups is shown in **Figure 1**. The time to failure is shown in **Figure 2**. About 90% of the failures occurred within three years. Given the 5-10 years design product life requirement, clearly creep corrosion has been causing early-life failures. The failures were predominantly on the PCBs (interconnects), followed by passive components and only a few failures on active components as shown in **Figure 3**. Of the creep corrosion failures on printed circuit boards, **Figure 4** shows that about two-thirds occurred on Pb-free PCBs and the rest on Pb-Sn PCBs. Creep corrosion was observed on non-soldered and in poorly soldered areas of the circuit boards. In these areas, the copper metallization and/or finish over the copper metallization was exposed to the environment. Lead-free soldered ImAg finished circuit boards suffered the most frequent creep corrosion failures. Failures were also reported for Pb-free soldered OSP finished circuit boards in harsh environments. The respondents reported that none of the failures are induced by overly aggressive design features. There was no clarity on the role of rework. The respondents had no standard test method to evaluate their products for susceptibility to creep corrosion.
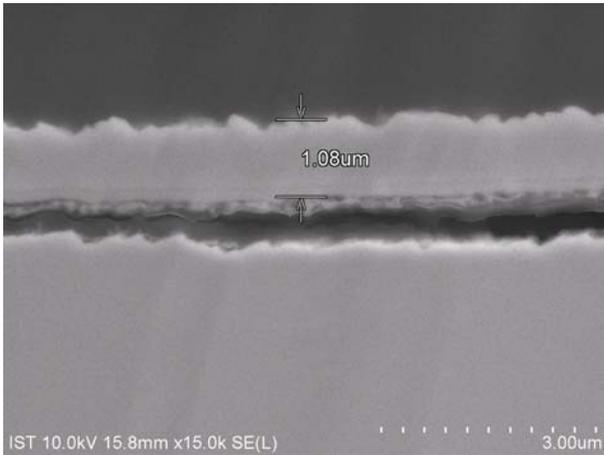
Figure 7: The thickness of the copper corrosion product grown on copper foil in the 2nd corrosion uniformity run (500 ppb H_2S environment) was about 1 μm in cross section as shown above and 0.94 μm from the weight gain measurement.

Tests based on MFG and on subjecting hardware to sulfur-bearing clays were not generally successful in predicting field creep corrosion failures. Failures were observed world wide, though the vast majority were in highly-polluted geographies and in industrial areas. All the respondents agreed that the failures were environmentally induced, attributing the failures mainly to the presence of sulfur-bearing gaseous contamination and high humidity. The role of flux was not clear. Four of eight respondents felt that flux residue played no role in the failures. The other half acknowledged that aggressive flux residues may have accelerated the creep corrosion.

Table 1: MFG test results

| Finish and wave solder flux	Corrosion	Edge corrosion	Creep corrosion severity	Electrical shorts detected, kΩ
ImAg + organic acid flux	Yes	No	High	5, 38, 0.6, 48, 1.5, 9.8, 3.6
ImAg + rosin flux	Yes	No	None	
OSP + organic acid flux	Yes	No	Low	
OSP + rosin flux	Yes	No	Low	
Pb-free HASL + organic acid flux	No	Yes	High (in isolated areas)	36
Pb-free HASL + rosin flux	No	Yes	None	
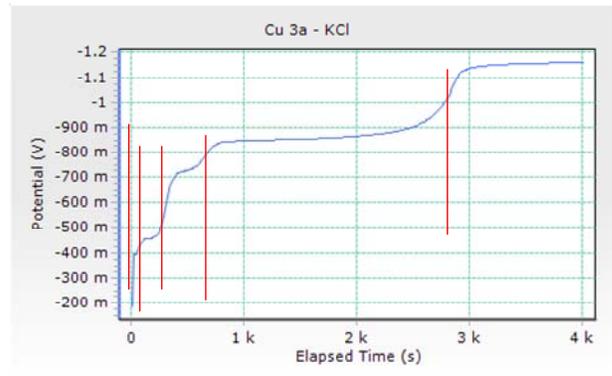
(a) Cu foil coulometric reduction
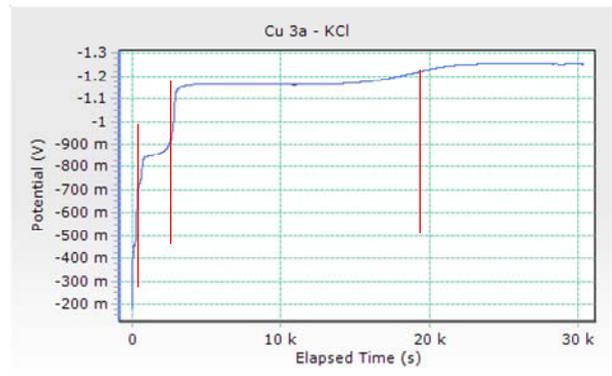
(b) Cu foil coulometric reduction
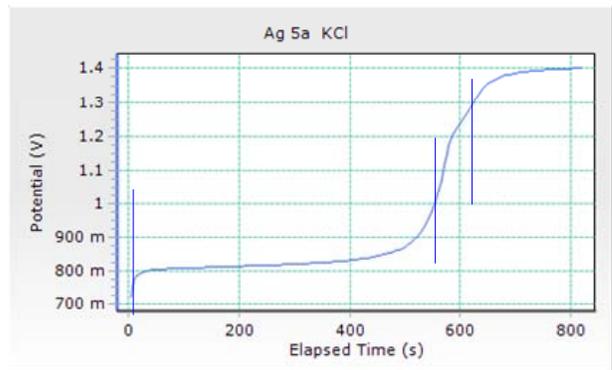
(c) Ag foil coulometric reduction

Figure 8: Coulometric reduction of metal foils of the 3rd corrosion uniformity run. The potential is versus saturated calomel electrode. The Cu corrosion products consists mainly of Cu_2S with very small amounts of Cu_2O and CuO. In Figure (a), the potential plateaus at 400-500 mV are unknown corrosion products; plateau at ~720 mV corresponds to ~25 nm Cu_2O; plateau at ~850 mV corresponds to ~90 nm CuO; and plateau at ~1170 mV corresponds to ~1360 nm Cu_2S. Figure (b) shows the same plot as in Figure (a), except that its time duration is 30k seconds to include the complete Cu_2S plateau at ~1170 mV. In Figure (c) the plateau at ~810 mV corresponds to ~55 nm Ag_2S.
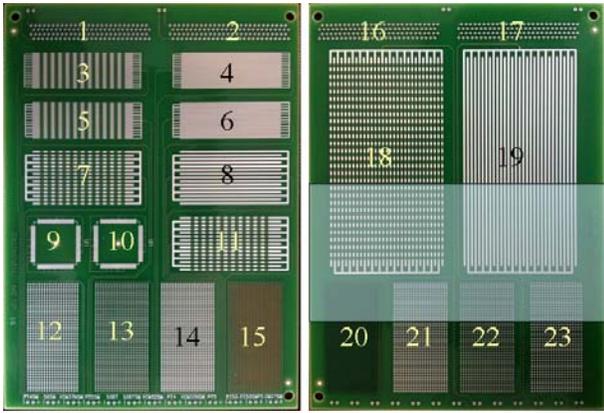
Figure 9: Numbered areas on test board are described in the text. The translucent blue box area was the area masked from the solder wave.

Figure 10: ImAg with wave soldering organic acid flux. Excessive corrosion occurred in the white ellipsed areas and creep corrosion in the red ellipsed areas.
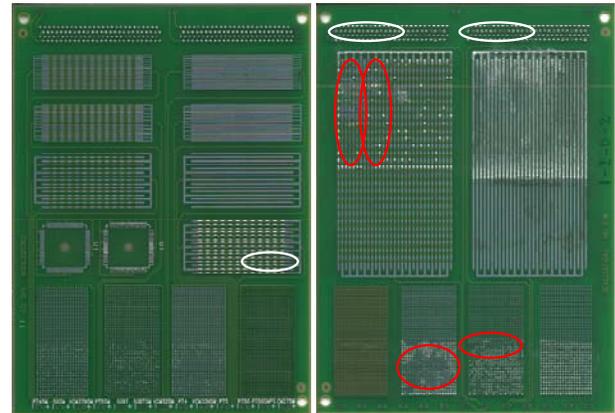
In phase 2, the iNEMI team discussed the creep corrosion failure mechanisms, mitigation methods, test methods to predict creep corrosion and product life in the field and environmental monitoring and control.

The purpose of phase 3, which is in process, is to understand the sensitivities of the already identified contributing factors, validating the effectiveness of some mitigation methods and to correlate experimental test conditions to environmental classification standards such as the ISA 71.04-1985 [6] and the silver and copper corrosion rate requirements described in the 2011 ASHRAE white paper [12]. This phase of the study involves laboratory based experiments to further investigate the sensitivities of the creep-corrosion influencing factors identified in phases 1 and 2. Three MFG test runs are planned, the first of which has been completed and is reported in this paper. The factors being studied include surface finish, flux type, solder mask geometry, solder paste coverage and reflow and wave soldering.

EXPERIMENTAL PROCEDURE AND RESULTS
The iNEMI phase 3 experiments began with establishing the spatial uniformity of corrosion and the rate of corrosion in a MFG chamber. The objective was to ensure that all the specimens hung in the chamber experienced similar corrosion rates. Once the uniformity of corrosion and target rate of corrosion of 500-600 nm/day had been achieved, the first of three tests on test boards with various finishes and two different wave-solder fluxes were run. The 2nd and 3rd test results will be reported in a later paper.
To test the spatial uniformity of corrosion in the chamber and achieve the target rate of 500-600 nm/day, 12 copper and 12 silver foils were hung on a rotary wheel in the top half of the MFG chamber and similarly oriented, but stationary foils were placed at the bottom of the chamber. Three spatial corrosion uniformity and corrosion rate tests were run. The test conditions for the first test run were as follows: H_2S =1700 ppb; NO_2 = 200 ppb; Cl_2 =20 ppb; SO_2 = 200 ppb; 40^oC; 70-75% relative humidity; 5 days duration. For the 2nd and the 3rd test runs, the H_2S concentration was changed to 500 ppb and 1000 ppb, respectively; all other conditions

remained unchanged. The total thickness of the corrosion products was measured by translating the rate of weight gain to corrosion rate, in terms of nm/day, using the approach described in Ref [12]. The corrosion rate values of the stationary foils at the bottom of the MFG camber varied widely from foil to foil. The corrosion rates of the metal foils hung on the rotating wheel in the top half of the chamber were quite tightly distributed as shown in **Figures 5 and 6**. These figures show one-standard deviation error bars. The worst-case standard deviation was for the case of 1700 ppb H_2S MFG environment: The standard deviation for the copper and silver corrosion rates was 59 and 24 nm/day, respectively.

The thickness of the corrosion products on some of the copper foils from the corrosion uniformity tests were measure by potting in epoxy, cross sectioning and polishing. **Figure 7** shows the cross section of a copper foil from the 2nd corrosion uniformity test. The energy dispersive analysis of the corrosion product shows high levels of Cu and S.

The chemistry of the corrosion products on the foils was determined electrochemically using coulometric reduction analysis: As shown in **Figure 8**, for metal foils from the 3rd corrosion uniformity run, the copper corrosion products consisted mainly of Cu_2S with very small amounts of Cu_2O and CuO. The silver corrosion product was only Ag_2S.
Based on the MFG test runs with H_2S concentrations of 500, 100 and 1700 ppb, the H_2S concentration for the MFG testing of the lead-free test PCBs was chosen to be 1200 ppb to achieve the target copper corrosion rate of 500-600 nm/day. In comparison, recent work by Xu [11] reported that all other factors being equal, 1500 ppb H_2S was required to achieve a copper corrosion rate of 500 nm/day.

Three MFG tests of lead-free test PCBs with various finishes are planned. The first test has been completed. The test circuit boards for the first test consisted of 1/2 ounce copper on top and bottom. Test boards were 140x110-mm by 1-mm thick. The FR4 epoxy used was compatible with
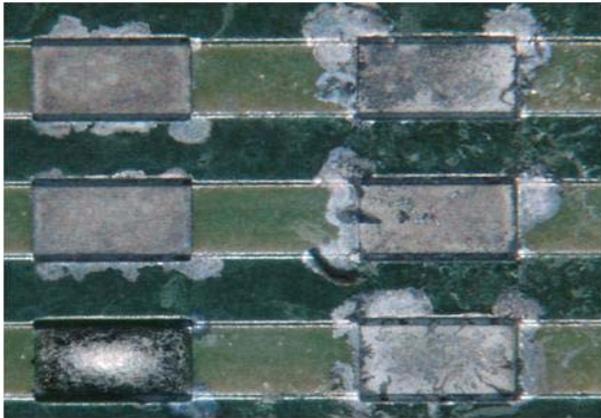
Figure 11: ImAg test board that was wave soldered with organic acid flux. Copper creep corrosion occurred in comb area with solder mask.

Figure 12: Pb-free HASL test board that was wave soldered with organic acid flux.

Pb-free soldering conditions. There were 23 areas on the board with various finishes and traces and vias with various pitches. The circuit board design made it convenient for visual inspection and electrical testing for creep corrosion. The areas on test PCBs shown in **Figure 9** are as follows:

- Areas 1 and 2 on the top side and areas 16 and 17 on the bottom side are plated-through holes with 1.5-mm pitch.
- Areas 3, 5 and 7 on top side are comb patterns with solder mask stripes: Area 3 has 0.23-mm traces on 0.4-mm pitch; area 5 has 0.30-mm traces on 0.5-mm pitch pitch; and area 7 has 0.66-mm traces on 1.27-mm pitch.
- Areas 4, 6 and 8 are same as 3, 5 and 7 but without the solder mask stripes.
- Areas 9 and 10 on top are 100 quad-flat pack (QFP). QFP at area 10 has Pb-free solder paste.
- Area 11 is same as area 7 but with Pb-free solder paste.
- Area 12, 13, 14 and 15 on top and 20, 21, 22 and 23 on bottom are 22r5 open via comb pattern on 0.94-mm pitch (0.38-mm pad to pad), 0.81-mm pitch (0.25-mm pad to pad 0.81-mm pitch (0.25-mm pad to pad) and 0.69-mm pitch (0.13-mm pad to pad), respectively.
- Areas 18 and 19 on bottom are comb pattern with 0.66-mm traces on 1.27-mm pitch. Area 18 has solder-mask stripes.

The 1st mixed-flowing gas test involved fabrication and testing of PCBs with three types of finishes:

- ImAg
- OSP and
- Pb-free HASL.

A 0.127-mm thick stencil was used to print the Pb-free solder paste on the comb pattern at area 11 and on the QFP at area 10 on the top side of the board. These were the only two areas of the test boards with solder paste. A rosin-based, low activity, halide-free, lead-free (ROL0) solder paste was used. The metallizations on the other areas of the top side of the boards had no solder cover. A common "tent" type or linear Pb-free reflow profile was used. The duration of temperature above $232^{o}C$ was 30 seconds with a peak temperature of $245^{o}C$.

After the Pb-free solder paste on the top side of the board had been reflowed, the bottom side of the board was wave soldered using a fixture to mask off the center part of the bottom side of the board, as shown in **Figure 9** to simulate the selective wave soldering condition. Because the fixture mask was not in intimate contact with the test boards, some flux invariably got under the fixture mask and contaminated the board. Two types of no-clean fluxes were used for the wave soldering operation: One was a low-activity rosin-containing flux; the other was a VOC-free, halide-free, rosin/resin free, organic activated flux. Flux was sprayed on the bottom side of the board just prior to the wave soldering. As in real production, some flux did flow through the unplugged vias to the top side of the board. The SAC305 (96.5% Sn ,3% Ag and 0.5% Cu) alloy was used with the solder pot temperature set at $265^{o}C$. The board pre-heat temperature before wave contact was $110^{o}C$ on top side of the printed circuit board, as specified for the fluxes.

The MFG test condition for the first test was as follows: H_2S =1200 ppb; NO_2 = 200 ppb; Cl_2 =20 ppb; SO_2 = 200 ppb; $40^{o}C$; 70-75% relative humidity; 20 days duration. The three types of board degradation observed were corrosion, edge corrosion and creep corrosion. Corrosion here refers to the general corrosion of the board metallization. Edge corrosion refers to the corrosion along the edge of the metallization. Creep corrosion refers to the corrosion products spreading on to the solder mask beyond the edges of the metallization. The MFG test results for the first run are listed in **Table 1**. Lead-free HASL boards were the only ones that did not suffer corrosion of the metallization. All the other boards had corrosion wherever the metallization was not covered with SAC solder. Edge corrosion was only seen on Pb-free HASL boards. Severe creep corrosion was observed on ImAg finished boards (**Figure 11**) and on isolated areas of Pb-free HASL boards that were wave soldered with organic acid flux (**Figure 12**). Some isolated low-level creep corrosion occurred on OSP boards that were wave soldered with rosin-based flux and with organic acid flux (**Figure 13**). The common denominator for severe creep corrosion was the use of organic acid wave solder flux. The occurrence of severe creep corrosion was

associated with high resistance electrical shorts as listed in **Table 1**.

DISCUSSION

The state of testing for creep corrosion is summed up by the following recent note from a reliability engineer at a major electronics hardware manufacturer: "The failure mode for the majority of the PCBs returned to me, that had failed in the field because of corrosion, failed by the growth of copper sulfide that spread out from the edge of the exposed copper metal. Copper sulfide is sufficiently electrically conductive to cause electrical shorting if it bridges adjacent solder pads. Even though the Battelle Class II caused heavy corrosion of copper, it did not accelerate the copper sulfide spreading. Finding the major variables that control the spreading of copper sulfide would be beneficial to the general electronics industry." The inability to reproduce creep corrosion in the laboratory using realistic acceleration tests was first pointed out by Xu et. al. to be due to creep corrosion being highly sensitive to surface chemistries **[10, 11]**.

The MFG environment used in this work and others is such that the rate of silver corrosion is about 1/25 the rate of copper corrosion (**Figures 5 and 6**); whereas, in data centers with known corrosion-related hardware failures, the rate of silver corrosion is typically about four time faster than that of copper corrosion (**Table 2**). In other words, the silver-to-copper corrosion rate ratio in data centers is ~ 25x4=100 times higher than that in the MFG chamber. Other researchers using MFG testing **[10, 11, 13]** have also reported much lower silver corrosion rates compared to copper. High relative humidity (70-75%) in the MFG chambers may be one explanation: Rice et.al **[13]** showed that copper corrosion rate rises strongly as a function of humidity; whereas, silver corrosion rate is not much affected by humidity.

The reason for the much higher copper corrosion rate in MFG environment as compared to the silver corrosion rate may be explained on the basis of how the corrosion kinetics of these metals are influenced by the H_2S concentration. Copper corrosion rate is more linearly dependent on the H_2S concentration; whereas silver corrosion rate plateaus off at higher H_2S concentration. One possible explanation for the relatively slower silver corrosion rate in air with high H_2S concentration may be that the silver sulfide growth rate is limited not by the availability of H_2S but by Ag^- ions not being able to diffuse to the surface of the corrosion product fast enough. In MFG testing, we use high H_2S concentrations to achieve targeted corrosion acceleration, which works for Cu but not Ag. Fortunately, creep corrosion field failure is

Table 2: Copper and silver corrosion rates in data centers that reported corrosion-related hardware failures in data centers in 2011. **[12].**

	Corrosion rate, nm/month		Ag/Cu corrosion rate ratio
	Silver	Copper	
Mean	76	30	3.8
Std dev	39	25	3.6
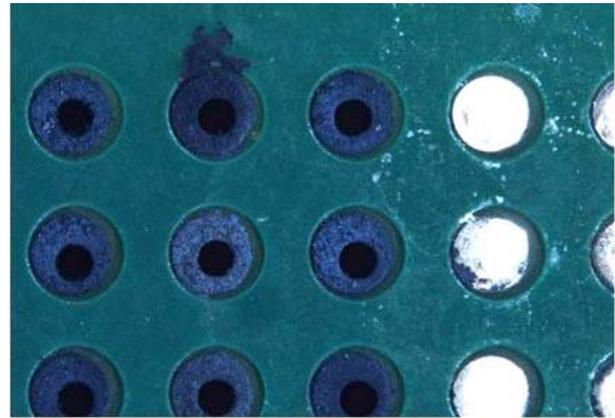
Figure 13: OSP test board that was wave soldered with organic acid flux.

due to copper sulfide; so MFG testing may be valid for predicting creep corrosion in the field.

Even though the predominant creeping corrosion product across all the surface finishes studied was copper sulfide, the extent of creep varied as a result of a multiple of contributing factors. In general, surface finishes like ImAg and OSP are relatively thin in comparison to Pb-Sn HASL or Pb-free HASL. ImAg, although good from a solder wettability perspective, is prone to galvanic corrosion. The standard electrode potentials of silver and copper are 0.8 V and 0.34 V, respectively. In locations where Cu is not completely coated by Ag (etch undercut locations), or exposed through porosity that typically exists in these thin coatings, a galvanic cell develops with Ag in the presence of humidity. In such a scenario, the cathodic silver galvanically corrodes the anodic copper. The issue with OSP is the thermal degradation of the polymeric layer during assembly. The porosity that results exposes the underlying copper to attack by sulfur-bearing gaseous contamination in the air. The corrosion on Pb-free HASL boards is primarily around the edge of the pads where the surface finish may not completely cover the copper and thus not be able to protect it from attack by the environment.

Creep corrosion of copper in environments rich in H_2S, a complex multi-step electrochemical chain reaction, has been studied by Kurella et. al. using TOF-SIMS depth profiling **[14]**. In the presence of moisture, H_2S dissociates into HS^- and then into S^{2--} along the adsorbed monolayers of water on the PCB surface. Copper ions react with S^{2-} ions resulting in the precipitation of Cu_2S. Depth profiling of the creeping corrosion product shows that the Cu^+ ions diffuse mostly laterally in the plane of the corrosion product while being reacted by the slower diffusing S^{2-} ions into the depth of the corrosion product. The Cu_2S corrosion product creeps along the PCB surface because the self diffusion of Cu^+ is significantly higher than that of S^{2-} in the Cu_2S layer **[15, 16]**. Cu^+ ions can diffuse quite far in the plane of the corrosion product before being reacted by S^{2-} ions to form Cu_2S.

TOF-SIMs depth profiling by Kurella et. al. has also shown that AgCl and CuCl that form in the presence of Cl^- ions are highly prone to migration along the surfaces of the PCB solder mask **[14].** The chlorides provide a medium through which or over which Cu^+ ions can migrate and subsequently react with S^{2-} ions forming Cu_2S. Depth profiling lends credence to this hypothesis by showing the sulfide layer creeping over the chloride layer covering the solder mask.

The present work has shown that the presence of organic acid flux residue is the single biggest contributor to copper creep corrosion. The test boards from the 2nd and 3rd MFG test runs will be studied using TOF-SIMS to understand the chemistry of the creep corrosion on PCB surfaces contaminated with organic acid flux residues.

CONCLUSIONS

ImAg, OSP and Pb-free HASL finished boards with reflowed Pb-free solder paste on the top side and wave soldered on the bottom side, some with no-clean organic acid flux and others with no-clean rosin-flux, were subjected to mixed-flowing gas environment with gaseous composition adjusted to achieve the targeted 500-600 nm/day copper corrosion rate. Copper creep corrosion was observed mainly on the ImAg finished boards that were wave soldered with no-clean organic acid flux. Pb-free HASL finished boards experienced some severe but localized creep corrosion due to exposed copper metallization. Creep corrosion was most severe in the wave soldered boundary areas where no-clean organic acid flux residue was present.

REFERENCES

[1] Directive 2002/95/EC of the European Parliament and of the council of 27 Jan 2003 on the restriction of the use of certain hazardous substances in electrical and electronic equipment.

[2] Cullen D. and O'Brien G., UL Laboratories, Implementation of immersion silver PCB surface finish in compliance with Underwriters Laboratories, IPC Printed Circuits Expo, 2004.

[3] Zhao P., Pecht, M., *"Field failure due to creep corrosion on components and palladium pre-plated leadframes,"* Microelectronics Reliability, 43 (2003) 775-783

[4] Veale R., Rockwell International, *"Reliability of PCB alternate surface finishes in a harsh industrial environment.* SMTA Int'l Proceedings, 2005.

[5] Abbott W.H., "The development and performance characteristics of mixed flowing gas test environment," IEEE Trans. of Component Hybrids and Manufactuirng Technology, vol. 11, no.1 . March 1988.

[6] ANSI/ISA-71.04-1985, *"Environmental Conditions for Process Measurement and Control Systems: Airborne Contaminants,"* ANSI/ISA-The Instrumentation, Systems, and Automation Society, 3 February 1986

[7] Cullen D., "Surface tarnish and creep corrosion on Pb-free circuit board surface finishes," IPC Works 2005.

[8] Mazurkiewicz P., HP Corp., "Accelerated corrosion of PCBs due to high levels of reduced sulfur gases in industrial environments," Proceedings of the 32nd ISTFA, Nov 12-16, 2006, Austin TX.

[9] Schueller R., *"Creep corrosion of lead-free printed circuit boards in high sulfur environments,"* SMTA Int'l Proceedings, Oct 2007.

[10] Xu C., Flemming D., Demerkin K., Derkits G., Franey J., Reents W., "Corrosion resistance of PWB surface finishes," APEX 2007.

[11] Xu C., Smetana J., Franey J., Guerra G., Fleming D., Reents W., Willie D., Garcia A., Encinas G., Xiaodong J., "Creep corrosion of PWB final finishes: Its cause and prevention," APEX 2009

[12] ASHRAE,"2011 Gaseous and particulate contamination guidelines for data centers," Atlanta, GA, ASHRAE 2011.

[13] Rice D.W., Peterson P., Rigby E.B., Phipps P.B.P., Cappell R.J. and Tremoureux R., J. Electrochem, Soc.: February I981, pg 27.

[14] Kurella A., Pathangey B., Wang Z., Ciarkowski T., "Analysis of Corrosion Films in Printed Circuit Assemblies," proceedings SMTAI 2011.

[15] Moya F., Moya-Gontier G.E., Cabane-Brouty F, Oudar J., Acta Metall., 1971, Vol 19, pg1189.

[16] Tereshkova S.G., Kinet. Catal., 1998, Vol 39, pg 217.